Biochimica et Biophysica Acta 1798 (2010) 105–113

Contents lists available at ScienceDirect

Biochimica et Biophysica Acta

journal homepage: www.elsevier.com/locate/bbamem

Backbone dynamics of the antifungal Psd1 pea defensin and its correlation with membrane interaction by NMR spectroscopy

Luciano Neves de Medeiros [a,b,1], Renata Angeli [b,1], Carolina G. Sarzedas [b], Eliana Barreto-Bergter [c], Ana Paula Valente [b,*], Eleonora Kurtenbach [a], Fabio C.L. Almeida [b,*]

[a] Instituto de Biofísica Carlos Chagas Filho, Programa de Biologia Molecular e Estrutural, Universidade Federal do Rio de Janeiro, Brazil
[b] Instituto de Bioquímica Médica, Programa de Biologia Estrutural, Universidade Federal do Rio de Janeiro, Brazil
[c] Instituto de Microbiologia, Universidade Federal do Rio de Janeiro, Centro de Ciências da Saúde, Cidade Universitária, 21941-900, Rio de Janeiro RJ, Brazil

ARTICLE INFO

Article history:
Received 15 April 2009
Received in revised form 25 June 2009
Accepted 8 July 2009
Available online 24 July 2009

Keywords:
Plant defensin
Membrane
Membrane protein
NMR
Dynamic
Lipari–Szabo
Antimicrobial
Fungus
Protein recognition
Membrane recognition
Transient interaction
Psd1
Antifungal

ABSTRACT

Plant defensins are cysteine-rich cationic peptides, components of the innate immune system. The antifungal sensitivity of certain exemplars was correlated to the level of complex glycosphingolipids in the membrane of fungi strains. Psd1 is a 46 amino acid residue defensin isolated from pea seeds which exhibit antifungal activity. Its structure is characterized by the so-called cysteine-stabilized α/β motif linked by three loops as determined by two-dimensional NMR. In the present work we explored the measurement of heteronuclear Nuclear Overhauser Effects, R1 and R2 ^{15}N relaxation ratios, and chemical shift to probe the backbone dynamics of Psd1 and its interaction with membrane mimetic systems with phosphatidylcholine (PC) or dodecylphosphocholine (DPC) with glucosylceramide (CMH) isolated from *Fusarium solani*. The calculated R2 values predicted a slow motion around the highly conserved among Gly12 residue and also in the region of the Turn3 His36–Trp38. The results showed that Psd1 interacts with vesicles of PC or PC:CMH in slightly different forms. The interaction was monitored by chemical shift perturbation and relaxation properties. Using this approach we could map the loops as the binding site of Psd1 with the membrane. The major binding epitope showed conformation exchange properties in the μs–ms timescale supporting the conformation selection as the binding mechanism. Moreover, the peptide corresponding to part of Loop1 (pepLoop1: Gly12 to Ser19) is also able to interact with DPC micelles acquiring a stable structure and in the presence of DPC:CMH the peptide changes to an extended conformation, exhibiting NOE mainly with the carbohydrate and ceramide parts of CMH.

1. Introduction

Defensins have been identified in many organisms from insect to humans, including plants. They play an important role in innate immunity against invading microorganisms. Defensins present a wide and distinctive antifungal and/or antibacterial spectrum of activity, suggesting their application as natural antimicotics and/or antibiotics [1,2]. Recently, the availability of complete genomes or transcriptomes has revealed a surprising abundance of genes encoding putative defensins [3,4]. They have been underestimated mainly because they share low similarity in the primary sequence but new bioinformatics techniques revealed the universe of defensin sequences [3]. The amount of coded proteins presumably protect against tolerance because it represents a dynamic strategy against pathogens. The biotechnological opportunity of defensin has been long recognized both as antibiotics for resistant strains and also expression in plant for crop protection [5–8].

Some important structural features can be identified by comparing the defensins: the majority shares the same cysteine-stabilized α/β motif, composed of three antiparallel β-strands and one α-helix. Their positive charge at physiological pH seems to be related to the initial interaction with anionic head groups of the microbial membrane lipids. The hydrophobic properties enable interaction with the core of the membrane that permits accommodation of the protein and consequently membrane disruption [9].

Different evidence have shown that the membrane permeation or disruption is only one among several mechanism involved but still the microbial membrane is the first barrier that should be overcome [7,9–11]. Thevissen et al. [12,13] proposed that

Abbreviations: CMH, monohexosylceramide; CSP, chemical shift perturbation; *Dm*AMP, *Dahlia merckii* antimicrobial peptide; DPC, dodecylphosphocholine; Het-NOE, Heteronuclear ^{15}N Nuclear Overhauser Enhancement; -M(IP)$_2$C), mannosyldiinositolphosphoryl-ceramide; pepLoop1, Gly12 to Ser19; Psd, *Pisum sativum* defensin; *Rs*AFP1, *Raphanus sativus* antifungal peptide; PC, L-α-phosphatidylcholine; PRE, paramagnetic relaxation enhancement; R1, heteronuclear longitudinal relaxation time; R2, heteronuclear transverse relaxation time

* Corresponding authors.
E-mail addresses: valente@cnrmn.bioqmed.ufrj.br (A.P. Valente), falmeida@cnrmn.bioqmed.ufrj.br (F.C.L. Almeida).

[1] Both authors contributed equally to this work.

0005-2736/$ – see front matter © 2009 Elsevier B.V. All rights reserved.
doi:10.1016/j.bbamem.2009.07.013

glucosylceramide present in fungus membrane is one important receptor for plant defensin binding. The blockage of glucosylceramide synthesis changes the fungus to a defensin-resistant form. Evidence from the literature demonstrated that patches of fungi membrane containing mannosyldiinositolphosphoryl-ceramide and glucosylceramides are selective binding sites for plant defensins *Dm*-AMP$_1$ and *Rs*-AFP$_2$ isolated from *Dahlia merckii* and *Raphanus sativus*, respectively [2,7,12,13].

Defensin mechanism of action is still unknown and the divergence in primary sequence hampers the identification of binding site and their mechanism of action being cysteines the only (clear) conserved amino acid. Recently a new feature was included in the analysis: dynamic properties.

The importance of protein dynamics in binding process has gained huge attention in the last few years. The possibility to measure movements in the ns to ms timescale has revealed the complexity of protein conformation ensemble in solution. [14,19,20]. Recent studies on protein dynamic have led to the realization that proteins are not structured in a unique conformation; rather, they frequently display regions undergoing conformational exchange. The novel view of binding and allostery takes into consideration the equilibrium among pre-existing conformational states of the protein before it encounters the ligand. In the ligand-bound form, no significant conformational transition is needed; instead, there is a population shift toward the ligand-bound conformational state. Several evidence have shown that regions displaying conformational diversity participate directly either in binding or in allosteric transitions [14–18].

The dynamics of the backbone of a protein can be monitored by Nuclear Magnetic Resonance (NMR) relaxation measurements, typically ^{15}N longitudinal relaxation (T1), transverse relaxation (T2), and ^{15}N–^{1}H heteronuclear NOE of a uniformly ^{15}N labeled protein. The relaxation measurements can be interpreted in terms of physical events, such as order parameters and correlation times, to obtain a hydrodynamic description of the protein by fitting data with the Lipari–Szabo model-free formalism [19–21]. Multiple timescales can be resolved, from seconds (real time measurements) to picoseconds. Movement on the pico- to nanosecond timescale corresponds to local and segmental motions whose energy barrier is below the thermal energy (kT) [19,20]. These are the so-called thermal motions. Overall rotational tumbling occurs on a timescale of tens of nanoseconds and is also thermally.

Our group used relaxation studies to access the importance of conformation selection for protein-membrane binding. We used PRE (paramagnetic relaxation enhancement) effect to investigate the conformation ensemble of PW2, an anticoccidal peptide selected by phage-display, with no stable structure in solution and that acquires different stable conformations in the presence of SDS and DPC micelles [22,23]. Cruzeiro-Silva et al. [24] showed that PW2 in solution is not completely flexible. The distances measured by PRE revealed the constrained motion in the aromatic region (Trp-Trp-Arg) and 10 ns molecular dynamic simulation in water showed the increase in order parameters in this same region. Measurements of relaxation dispersion pointed the amino acids in exchange and they locate close to the WWR motif. Interesting to note that the aromatic region is the consensus among different peptides in the phage-display selection process [25].

In this work we assessed the defensin–membrane interaction using *Pisum sativum* defensin 1 (Psd1) as our model [26]. Psd1 exhibit high antimicrobial activity against specific fungi, including pea pathogens, but not against bacteria [26]. The solution structure of Psd1 was determined by high-resolution NMR spectroscopy [27]. Psd1 adopts a typical cysteine-stabilized α/β motif, composed of three antiparallel β-strands and one α-helix. The secondary elements are joined by two loops and one turn (Ala7-Asn17, Ala28-Ile31 and His36-Trp38) and those were the less defined regions in the calculated structure [27]. The recombinant Psd1 was acquired at high levels in *Pichia pastoris* expression system [28] and it exhibit the same structural and functional properties as the native one.

We have used NMR to analyze the conformation and dynamics of rPsd1 in the presence of vesicles containing phosphatidylcholine (PC) and a mix of PC with glycosphingolipid extracted from hyphae of *Fusarium solani* (CMH). We also investigated the effect of DPC micelles with or without CMH. The results showed that Psd1 interacts with vesicles of PC or PC:CMH in slightly different manner. The interaction was monitored by chemical shift perturbation and relaxation properties. Using this approach we could map the loops as the binding site of Psd1 with the membrane. The major binding epitope showed conformation exchange properties in the μs–ms timescale supporting the conformation selection as the binding mechanism. Moreover, the peptide corresponding to this loop is also able to interact with DPC micelles acquiring a stable structure and in the presence of DPC:CMH the peptide change to an extended conformation, exhibiting NOE mainly with the carbohydrate and ceramide parts of CMH. This is in accordance with previous studies showing the fragments of defensins presents antimicrobial activity [29–31].

2. Materials and methods

L-α-phosphatidylcholine (PC) from egg yolk was purchased from Avantis Corp.; Perdeuteretade D38-dodecylphosphocholine (DPC) and $^{15}NH_4Cl$ was purchased from Cambridge Isotope Laboratory; Monohexosylceramide (CMH) from *F. solani* was isolated as described by Duarte et al. [32]. All other chemicals were purchased from Sigma Chemical (St. Louis, MO, USA). All products were of analytical grade.

2.1. P. pastoris expression and purification of ^{15}N Psd1

Psd1 was expressed and purified as described elsewhere [26]. Briefly, Psd1-expressing *P. pastoris* colony was grown in minimal glycerol medium (BMG) for approximately 24 h at 28 °C and for 18 h at 30 °C with constant shaking. These cultures were centrifuged and the cell mass was resuspended in BBS medium containing 0.7% methanol and 4 g/L $^{15}NH_4Cl$. The induction of rPsd1 synthesis was carried out for 120 h by daily supplementation of 0.7% methanol. The crude culture was applied to a Toyopearl SP-650 M column. The peak containing proteins with low molecular weights was pooled and purified by semipreparative reversed-phase HPLC on a Vydac C8 column (208TP510). The fractions collected were dried under vacuum and dissolved in milli-Q water.

2.2. Vesicle preparation

Large unilamellar vesicles (LUV, 100 nm in diameter) were prepared according to the extrusion method of [33]. PC (3.8 mg) or PC:CMH (9:1 ratio containing 3.42 mg PC and 0.37 mg CMH) were dissolved in 200 μL of chloroform, dried under a stream of nitrogen and hydrated in 1 mL of 20 mM sodium phosphate buffer and 20 mM sodium chloride. The final concentration of PC or PC:CMH was 5 mM. Extrusion was done 40 times through stacked polycarbonate filters with a pore size of 0.1 μm.

2.3. NMR spectroscopy

All experiments were carried out at 25 °C on a Bruker DRX-600 spectrometer. Water suppression was achieved using the WATERGATE technique [34,35].

2.3.1. Relaxation parameters

^{15}N relaxation measurements were acquired using two-dimensional, proton-detected heteronuclear NMR experiments, for each of assigned

amide nitrogen implementing standard pulse sequences based on Farrow et al. [36]. T1, T2 and NOE spectra were recorded with spectral widths of 1024×256 points in the ^{1}H and ^{15}N dimensions. The field strength of the CPMG refocusing train was 3.3 kHz and a 1.2 ms delay was used between the refocusing pulses [37,38]. The effects of cross relaxation between ^{1}H–^{15}N dipolar and ^{15}N chemical shift anisotropy were removed applying ^{1}H 180° pulses during relaxation delays [39]. The relaxation delay for T1 and T2 measurements was 4 and 2 s, respectively. T1 values were measured in a series of spectra with relaxation delays of 0.020 s; 0.050 s; 0.100 s; 0.200 s; 0.300 s; 0.400 s; 0.500 s; 0.700 s; 0.900 s; 1.000 s; and 1.250 s. T2 measurements were taken with relaxation delays of 0.010 s; 0.025 s; 0.050 s; 0.075 s; 0.100 s; 0.125 s; 0.150 s; 0.175 s; 0.200 s; 0.250 s; and 0.300 s. To allow NOE evolution, ^{1}H–^{15}N steady-state NOE values were measured with two different data sets, one collected with no initial proton saturation and a second with initial proton saturation. The proton saturation period was 5 s.

2.3.2. Model-free calculations

Relaxation parameters were fitted according to Lipari–Sazabo model-free formalism to extract the intramolecular dynamics. We have used the software Model-free (v. 4.0) [19,40], from Arthur G. Palmer III research group. We used R1, R2, and NOE relaxation parameters and an axially symmetric diffusion model. The estimates of the overall correlation time τ_m was obtained using the R2/R1 ratio mean in a Monte-Carlo simulation.

2.3.3. Psd1 in PC and PC:CMH vesicles

Chemical shift perturbation (CSP) spectra were obtained using ^{1}H–^{15}N heteronuclear single quantum coherence (HSQC) spectra with 1024 points×256 points. NMR spectra were recorded on 0.5 mL samples of 50–200 μM ^{15}N-labeled Psd1 in 20 mM sodium phosphate buffer pH 5.0 and 20 mM sodium chloride in the presence or absence of 5 mM PC or PC:CMH (9:1, molar ratio) vesicles. The chemical shift perturbation was evaluated by the following equation: $\Delta\delta = (\Delta\delta_H^2 + \Delta\delta_N^2/10)^{1/2}$ in ppm, and $\Delta\delta_H$ or $\Delta\delta_N$ equal δ_H or δ_N of Psd1 in presence of vesicles less δ_H or δ_N of *P*sd1 free in solution.

2.3.4. Psd1 or pepLoop1 in DPC and DPC:CMH micelles

Psd1 (160 μM) or pepLoop1 (3.6 mM) were dissolved in 300 mM DPC, 40 mM sodium phosphate buffer (pH 5.5) and 10% D2O. DPC: CMH samples were prepared by adding dry weight of CMH to the DPC/protein or peptide sample. Psd1:CMH molar ratio was 1:10 and pepLoop1/CMH was analyzed in two molar ratios 0.5: 1 and 3:1.

2.3.5. PepLoop1 structural calculations

The peptide pepLoop1 (GVSFTNAS) was synthesized by Genemed Synthesis Inc at 95% purity and certified by mass spectrometry. For pepLoop1 in DPC, the structure were calculated using CNS_solve v.1.1 using a set of 300 distance restraints derived from a NOESY spectra acquired in a Bruker Avance III 800 MHz. The peptide was fully assigned using a combination of NOESY and TOCSY spectra; three NOESY spectra were acquired at 100 ms, 150 ms and 200 ms; we used the 200 ms NOESY for structural calculation. No spin diffusion was observed at this mixing time. For the peptide in DPC plus CMH using pepLoop1:CMH molar ratio of 3:1, we used CNS_solve v 1.1 with a set of 80 NOEs most of them sequential NOEs. We also use dihedral restraints derived from $^{3}J_{HNH\alpha}$. According to Fig. 6, when $^{3}J_{HNH\alpha}$ was higher than 8 Hz we used the phi angle restrained to from 90° to 150°. The $^{3}J_{HNH\alpha}$ was measured using the splitting of the NOESY spectra processed using Gaussian Multiplication window functions. For the sample DPC plus CMH using pepLoop1:CMH molar ratio of 3:1 we also run a COSY spectrum. For the structure statistics see supplementary Table 1.

3. Results

3.1. Psd1 backbone dynamics in the free state

The backbone dynamics of rPsd1 have been determined through solution NMR measurements of relaxation parameters R1, R2 and steady-state NOE of the amide group resonances. Fig. 1 shows the relaxation measurements values for the rPsd1 amino acid residues. Most of Psd1 residues showed similar values for R1, R2 and NOE compatible with the defensin fold and therefore stable secondary structure elements. Gly12 is the only residue that showed reduced

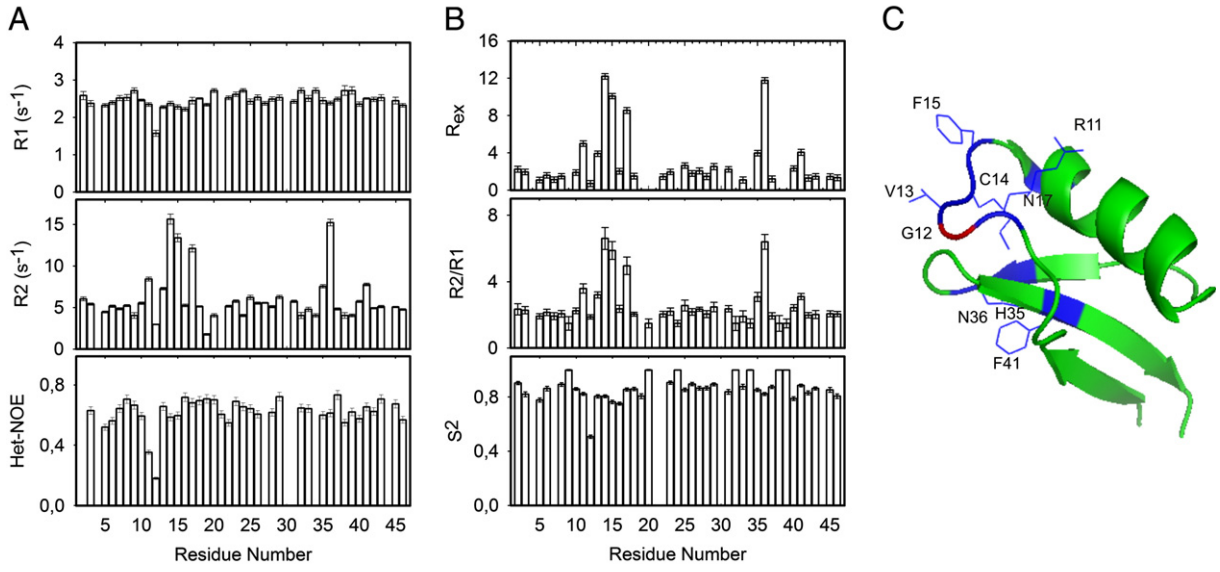

Fig. 1. ^{15}N backbone relaxation measurements for Psd1 free in solution. (A) R1, R2, and $^{1}H/^{15}N$ heteronuclear NOE plotted as a function of the residue number for *P*sd1. Values of R1 and R2 were obtained from the fit as single exponential decay of the time dependence of the relaxation data measured. The error bars indicate the fitting error. The absence of bars indicates that the values could not be accurately measured due to overlaps. (B) Lipari–Szabo model-free analysis of ^{15}N relaxation data of Psd1. The figure shows Rex, R2/R1 and order parameter (S^2) plotted as a function of the residue number for Psd1. The experiments were run at 25 °C. (C) Ribbon representation of Psd1 highlighting the side chains of the residues in conformational exchange in blue and the flexible hinge Gly12 in red. Gly12 is the only residue with decreased order parameter, showing thermal flexibility.

values of R1, R2 and HNNOE, indicating the presence of motion in the timescale of picoseconds. R2 values in the first loop (Ala7-Asn17) and Turn3 (His36-Trp38) showed bigger values than the average, typical of internal motion in μs–ms time scale.

We used the extended Lipari–Szabo model-free formalism to obtain the order parameter (S^2), that describe the presence of thermal motion and the residues involved in conformational exchange, undergoing motions timescale μs–ms (Rex). High values (0.87) observed in S^2 indicated significant restriction of the fast motion of the amide bond vector (N–H vector), consistent with well-organized Psd1 structure. Gly12 is the only exception, showing thermal motion with an order parameter of 0.51. The extended model, with the inclusion of the parameter Rex, was necessary to correctly describe the dynamics around the loops, especially Loop1 (from Ala7 to Asn17) and Turn3 (from His36 to Trp38). The isotropic overall correlation time was 5.0 ns, consistent with the monomeric form of the protein.

Another way to find the presence of conformational exchange is by analysis of R2/R1 ratio. Values of R2/R1 bigger than the average value can be readily attributed to conformational exchange, especially for Psd1 as shown in Fig. 2. In the present manuscript we will use R2/R1 ratio to compare the milli- to microsecond motion between Psd1 free in solution and in the presence of phospholipid vesicles. The advantage of using this ratio is that it does not depend on any model or fitting. This is an important advantage since it is not trivial to describe the hydrodynamic motion of Psd1 in rapid exchange between the free and vesicle-bound form.

Both the fitting of Rex by using the extended Lipari–Szabo model-free formalism or by looking at R2/R1 values indicated the presence conformational variability in Loop1 and Turn3, with the exchange between conformers in the micro- or millisecond time scale. The residues in Loop1 that exhibited significant conformational exchange were Arg11, Val13, Cys14, Phe15 and Asn17, resulting in positive values of Rex and residues Cys35 and His36, close to Turn3. The correlated motion between Loop1 and Turn3 is not surprising, since they are connected via disulfide bond (Cys14-Cys35). Fig. 1 shows the ribbon representation of Psd1 where the amino acids with conformational exchange (high Rex) were colored in blue and the Gly12 in red. Note that the residues in conformation exchange are close to each other forming a patch in Psd1 structure. Gly12 displayed thermal motion, which occurs in the timescale of pico- to nanoseconds, acting as a hinge in the middle of the loop in conformational exchange. This hinge motion of Gly12 plays an important role in the loop dynamic properties; it is worth mentioning that this residue is highly conserved among plant defensins.

3.2. Psd1 interaction with vesicles of PC and PC:CMH: chemical shift perturbation

We used chemical shift perturbation (CSP) to monitor rPsd1 interaction with PC and PC:CMH vesicles. We acquired HSQC spectra of the ^{15}N labeled rPsd1 free and in the presence of vesicles prepared with PC and PC:CMH (molar ratio 9:1). Fig. 2 shows the difference in chemical shift observed for the amide group for the free protein and in the presence of vesicle of PC (black bars) and PC: CMH (white and red bars).

The changes in chemical shift indicated that rPsd1 interacts with PC and PC:CMH vesicles causing similar CSP. Since the line width did not increase significantly, we could also infer that Psd1 interacts in fast exchange with the PC vesicle. Similar regions were probed by both systems, and bigger changes were observed around Loop1 and helix1 in the presence of both PC and PC:CMH. The line in Fig. 2 shows the limit of one standard deviation. In Fig. 2 the residues with CSP above the line are highlighted. Note that the perturbed regions are predominantly positive (Fig. 2), mainly due to Arg11, His23 and Lys27 residues. This indicates that Coulombic attraction is very important for the interaction of Psd1 with PC vesicles, as expected. This data suggested that Psd1 might slide freely in the PC bi-dimensional interface. The increase in salt concentration led to a decrease in CSP values, tending to the chemical shift values of the free state (not shown). The salt dependence reinforce that the Coulombic attraction as the first binding event.

Also CSP decreases with the increase of protein concentration, showing a saturation behavior. The effect showed in Fig. 2 tends to vanish at Psd1 concentration above 200 μM and lipid concentration of 5 mM. All the experiments of CSP in the present manuscript are done at non-saturant concentrations of Psd1 (50 μM).

Since PC comprises the vast majority of the PC:CMH vesicle surface (~90%), it was expected that the absolute value of CSP was predominantly due to the contact with PC. Nevertheless, significant differences were observed comparing the CSP in the presence of PC (black bars) and PC:CMH (white and red bars). To further analyze these differences we looked at residues that exhibited changes in CSP greater than 100% when compared with PC only (Fig. 2, red bars). They are highlighted in red in Fig. 2. The presence of CMH in the bilayer generated perturbation in the residues located at loop regions, especially those in Loop1 and Turn3. Remarkably, several cysteines changed in the presence of CMH indicating a conformation accommodation of Psd1 in this type of vesicle. Overall we believe that the main perturbation was probably due to non-specific electrostatic interaction with PC, while changes generated by the presence of CMH involve other type of interactions such as hydrogen bonds (Thr16 and Asn17 among others) and hydrophobic interactions with residues Val13, Phe15, Ala18 and Trp38.

3.3. Psd1 interaction with vesicles of PC and PC:CMH: dynamic properties

To further investigate the interaction of Psd1 with membranes we compared the R2/R1 ratio observed in the free state and in the presence of PC:CMH vesicles, since it has a relationship with overall rotational correlation time, τ_m, and motions in μs–ms timescale [40]. The R2/R1 ratio of the each residue for Psd1 free solution was very similar in all protein, with an average value around 2.15 (Fig. 3). The residues around the first loop and the Turn3 (Ala7-Asn17 and His36-Trp38) had bigger R2/R1 values when compared to the average, compatible with exchange processes.

The presence of PC:CMH vesicles induced several changes in the R2/R1 ratio. Amino acids Cys14, Phe15 and His36 had a decrease in R2/R1 ratio (Fig. 3, red). In opposition, residues Asn17, His29, His36, Asn37 and Trp38 had an increase in the R2/R1 ratio (Fig. 3, magenta). As expected, the amino acids with that presented bigger changes co-localize in the first loop and Turn3 region.

Here, we used the information from R2/R1 ratio solely as a way to map the site of interaction of Psd1 with PC:CMH (Fig 3B). Since binding can induce restriction of motion of a certain regions of a protein, stabilizing one particular conformer [14]. This conformational selection leads to a decrease in Rex, as observed for residues Cys14, Phe15 and His36. On the other hand, transient binding can induce an increase in Rex, since the ligand can be in exchange between its free and bound conformation. The binding of Psd1 to PC:CMH vesicle can evoke both effect in Rex. Probably, conformational selection is taking place, but the transient binding prevent us to fully analyze this data. To completely understand this phenomenon we need further data and this is not the main purpose of this manuscript.

3.4. Psd1 interaction with micelles of DPC: chemical shift perturbation and dynamic properties

The use of vesicles for solution NMR studies is restricted to systems in fast exchange; otherwise the resonances would be broadened. Micelles are the alternative system for membrane protein studies. We decided to investigate the changes in chemical

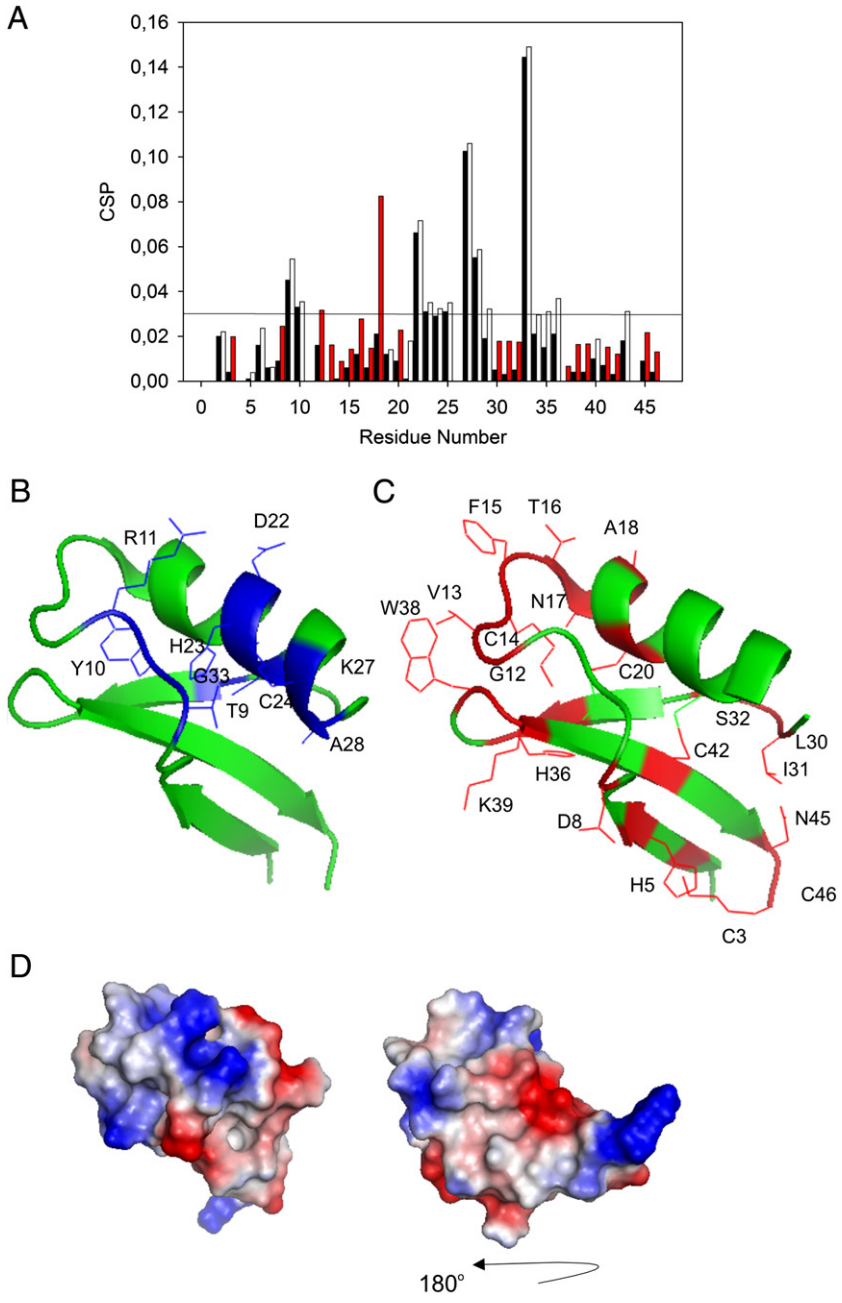

Fig. 2. Chemical shift perturbation (CSP) of Psd1 in the presence of vesicles of PC and PC:CMH (9:1) (A). CSP was obtained according to the equation shown in the Materials and methods section. The horizontal line shows the limit of one standard deviation. To map CSP evoked by the presence of PC, we considered significant CSP above one standard deviation (above the line). Sample condition was as following: 50 μM [Psd1], 20 mM phosphate buffer pH 5.0 plus 20 mM NaCl. Black bars refer to chemical shift perturbation in the presence of PC vesicles and white/red bars in the presence of PC:CMH (9:1) vesicles. The residues that were perturbed by PC:CMH (9:1) in more that 100% relative to PC only were colored in red bars. (B) Ribbon representation of Psd1 highlighting in blue the CSP evoked by the presence of PC vesicles. (C) Ribbon representation of Psd1 highlighting in red the CSP evoked by the presence of CMH. These residues were also colored as red bars in A. (D) Electrostatic potential surface of Psd1. Blue are positive, red are negative and white neutral residues. The structure shown in the left are in the exact same orientation as in B and C. In the right it was rotated by 180°.

shift of rPsd1 in the presence of micelles of DPC and DPC CMH. Fig. 4 shows the CSP when chemical shift values in the presence of compared to rPsd1 in the free state. The residues that were perturbed above one standard deviation were colored in magenta (Fig. 4). Residues that the resonances are broadened beyond detection are shown in red (Fig. 4). The same regions probed by the experiments with phospholipid vesicles were also monitored with DPC micelles: Loop1 and Turn3. Furthermore, the changes observed extend the ones in vesicles, probably because due to micelle properties the rPsd1 binding equilibrium is shifted toward the bound state. It is possible to speculate that in micelles, due to different dynamics (faster) and bigger curvature, the hydrophobic aliphatic chains are more exposed leading to bigger Psd1 insertion.

3.5. PepLoop1 (Gly12-Val13-Ser14-Phe15-Thr16-Asn17-Ala18-Ser19) structure in DPC and DPC:CMH

Based on the mapped specific interaction with CMH we synthesized pepLoop1. PepLoop1 comprises the residues that were perturbed by the presence of CMH. Fragments of a given protein do not necessarily display the same conformation when it is free in solution. However, they maintain the interaction properties, often

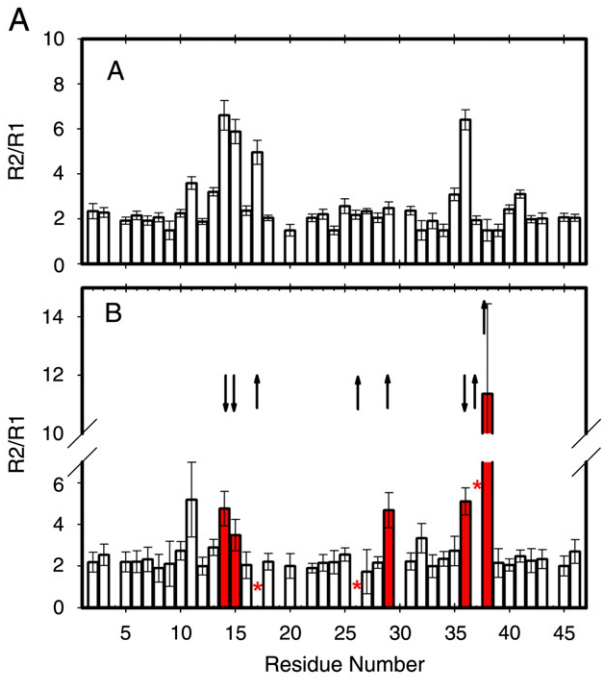

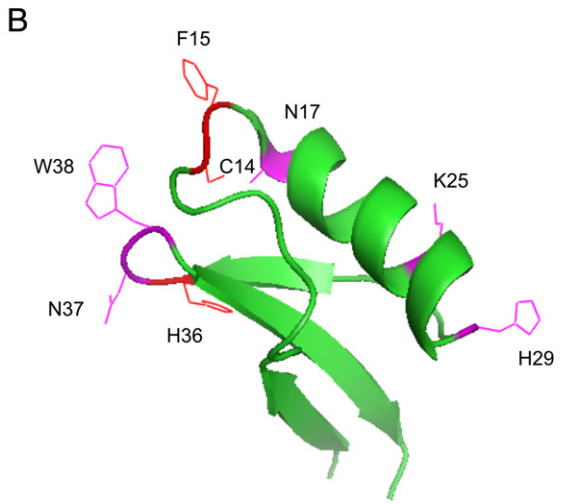

Fig. 3. (A) R2/R1 ratio for each amide ^{15}N of Psd1 (top), values obtained for Psd1 free in solution, the same shown in Fig. 1; (bottom), values obtained for *P*sd1 in the presence of PC:CMH (9:1) vesicles. The experiments were performed with extruded vesicles prepared with 20 mM phosphate pH 5, 20 mM NaCl, 200 μM Psd1 and 5 mM total lipids. The error bars are the sum of the fitting error from R1 and R2. The bars in red highlight the residues with significant difference in R2/R1. We considered significant when the observed difference in R2/R1 ratio are bigger than the sum of the error. The red asterisk indicates the residues where R2/R1 ratio could not be measured due to broadening of the line beyond detection. These residues are in conformational exchange. The arrow indicates the increase or decrease of conformational exchange. The absence of bars indicates that the values could not be accurately measured due to overlaps. (B) Ribbon representation of Psd1 highlighting the residues where conformation exchange were modified by the presence of PC:CMH (9:1) vesicles. Increase in conformational exchange is in magenta and decrease in red. Note that both reflect binding.

with lower affinities. One explanation is that the peptide free in solution is in equilibrium among several conformations and upon interaction the interacting-conformer is stabilized [14,18,24]. Based on this assumption, we mapped the specific interaction with CMH using pepLoop1.

Loop1 extends from residue 7 to 17 and appears as the most important membrane binding site. We decided to synthesize pepLoop1 starting from Gly12, since it is the flexible hinge of Loop1. To facilitate the experimental procedure we switched Cys14 to Ser14 in the synthetic peptide. Next we probe the interaction of pepLoop1 with DPC and DPC:CMH. The peptide sequence is the following: Gly12-Val13-Ser14-Phe15-Thr16-Asn17-Ala18-Ser19.

PepLoop1 did not have stable structure in solution but was stabilized in the presence of DPC micelles. Interesting for such small peptide, its structure converged as shown in Fig. 6A. The side chain of Ser14, Phe15 and Thr16 are well converged. Val13, Phe15 and Ala18 form a hydrophobic surface, probably facing the micelle, while Thr16 seems to be interacting with the polar head group.

Fig. 5A shows the observed NOEs for pepLoop1 in DPC micelles. Several medium and long range connectivities were observed. The long range NOE between Val13 and Ala 18 imposed a slight bend in the peptide.

When the micelles were mixed with CMH, there was a big change in the NOE profile and scalar coupling values ($^3J_{HNH\alpha}$). Fig. 6B shows the calculated structure for the new set of NOEs and the observed scalar coupling ($^3J_{HNH\alpha}$). It is worth mentioning that in the presence of CMH $^3J_{HNH\alpha}$ ranged from 7 to 15 Hz in the region Val13-Ans17, indicative of an extended conformation.

Fig. 5B shows the observed NOEs for pepLoop1 in the presence of DPC:CMH (0.5:1 — CMH:pepLoop1) and Fig. 5C DPC:CMH (3:1 —

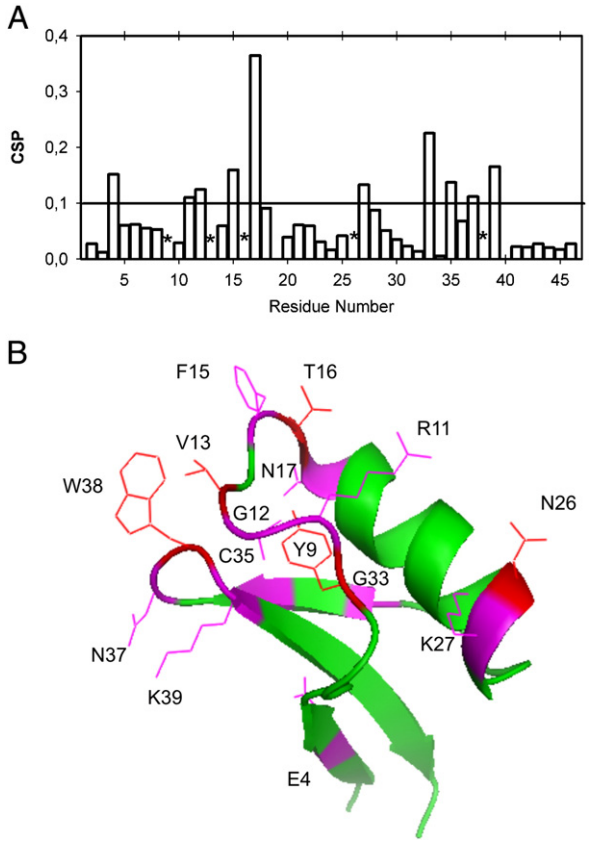

Fig. 4. (A) Chemical shift perturbation of Psd1 by the presence if DPC micelles and DPC micelles plus CMH, respecting a molar ratio CMH:Psd1 1:10. The presence of CMH did not show any change in the HSQC spectrum. The CSP plot refers to both conditions. The sample condition was as follows: 160 μM [Psd1] in 20 mM phosphate buffer pH 5.0 plus, 20 mM NaCl, 300 mM DPC. In the sample containing CMH, we added 600 μM of CMH. The horizontal line shows the limit of one standard deviation. To map CSP evoked by the presence of DPC or DPC plus CMH, we considered significant CSPs above one standard deviation (above the line). The black asterisks shows residue with broadening of the line beyond detection. These residues are in conformational exchange. (B) Ribbon representation of Psd1 highlighted in magenta shows the residues with significant CSP. In red are the residues that vanished from the spectra indicating that the presence of DPC significantly increased conformational exchange.

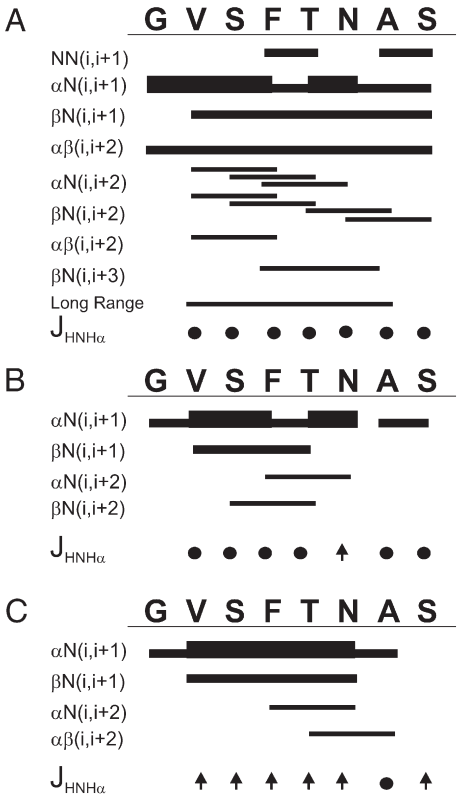

Fig. 5. Summary of NOEs of pepLoop1 in DPC micelles (A) or DPC plus CMH, respecting the CMH:pepLoop1 molar ratio of 0.5:1 (B) and 3:1 (C). The data were extracted from NOESY spectra with mixing time of 150 ms. All experiments were carried out at 3.6 mM pepLoop1, 20 mM phosphate buffer and 300 mM DPC.

CMH:pepLoop1). There was a decrease in the number of NOEs when compared with the peptide in DPC. This is probably due to the adoption of an extended conformation in the presence of CMH. The long range NOE between Val13 and Ala18 observed for the peptide in DPC was not observed in the presence of CMH. The structural statistics are shown in Supplementary Table 1.]

Moreover, several NOEs between pepLoop1 and CMH were observed (Fig. 7). CMH was re-assigned in DPC based on previously published values [32]. Phe15 aromatic δ protons showed NOEs with the ceramide part of CMH and Thr16 β protons showed several unambiguous NOEs with the glycosil part of CMH. These data suggest that Psd1 is interacting with the surface of the micelle.

4. Discussion

4.1. Identification of minimal domains in defensins

Several strategies have been used to identify minimal active domains of defensins in an attempt to create new antimicrobial agents [29–31,41]. Peptides derived from full length proteins are sometimes even more potent than the source. The MBG01 peptide (19-mer) deduced from *Raphanus* defensin Rs-AFP2, that corresponds to the β2–β3 loop was synthesized and its cysteines replaced by α-aminobutyric acid [31]. The derived peptide showed improved antifungal activity when compared to the native defensin (lower MIC value). Interesting, this peptide also has a Phe and a Val in the loop region. Vila-Perelló et al. [29,30] synthesized 13- to 19-mer peptides based on a thionin from *Pyrularia pubera* and the resulting peptides showed an antimicrobial activity similar to the native thionin. Here we showed that pepLoop1 binds CMH, helping us to contribute toward the elucidation of the binding mechanism of Psd1 to fungal membranes. For now we do not know if this peptide shows antimicrobial activity. Studies with peptides, including pepLoop1, corroborate the assumption that fragments of defensins conserve the interaction properties.

Similar results were observed for human defensins where the three-dimensional structure is not always important for antimicrobial activity since the replacement of cysteines by α-aminobutyric acid does not interfere in the antibacterial activity but changes chemotatic properties of the protein [42]. On the other hand, it is not clear if this is always the case. The presence of cysteines and, thus the correct fold, seems to be important for many of the activities of defensins [43,44].

Summarizing, these results suggest that specific region in the defensins is responsible for activity and that includes the ability to interact with membranes and other parts of defensins are responsible for specific recognition and anchoring to the membrane.

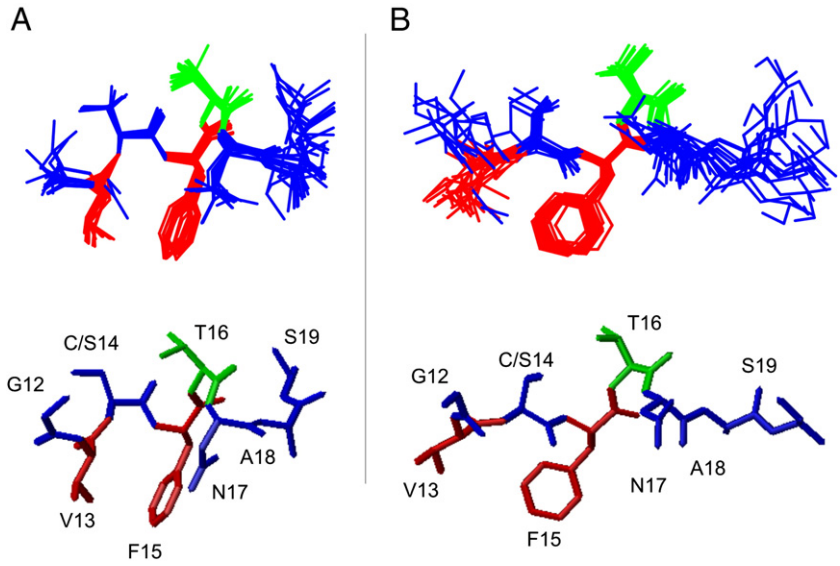

Fig. 6. Superposition of the 15 lowest energy structures of pepLoop1 in the presence of DPC (A, top) and DPC plus CMH, respecting a molar ratio CMH:pepLoop1 3:1 (B, top). pepLoop1 sample (3.6 mM) was prepared in 300 mM DPC, 20 mM sodium phosphate buffer (pH 5.5), 10% D_2O and DPC:CMH samples were prepared by adding dry weight of CMH to the DPC sample. In the bottom it shows a representative of the ensemble for each of the structures.

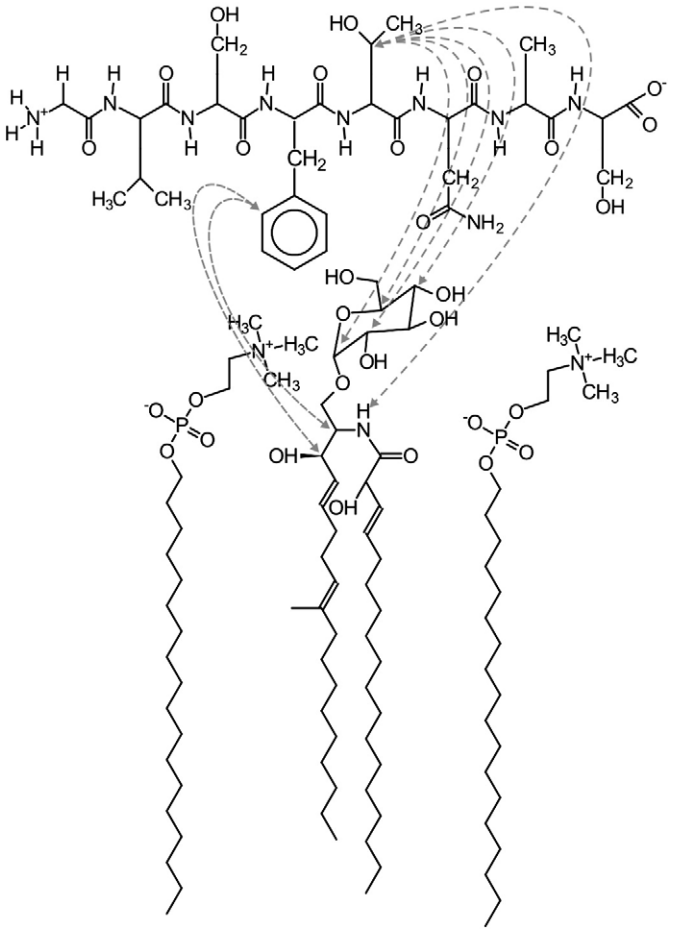

Fig. 7. Representation of pepLoop1, two DPC monomers and one CMH. The arrows shows the observed intermolecular NOEs obtained from a NOESY spectrum with mixing time of 150 ms. All experiments were carried out at 3.6 mM pepLoop1, 20 mM phosphate buffer and 300 mM DPC and 10.8 mM CMH (CMH:pepLoop1 molar ratio of 3:1). Note that the interaction of the peptide with CMH occurred through the contact of Phe15 side chain with the aliphatic chains and Thr16 with the carbohydrate group, possibly making hydrogen bonds. We could not observe intermolecular NOEs with DPC, possibly because it is only 1% protonated.

There are features of the primary sequences of plant defensins that are important to comment with perspective of the results showed in this manuscript. We compared the primary sequence of Psd1 with other defensins, focusing the ones from the same family and tribe. Defensins that are evolutionary related may maintain the mechanism of action and their interaction target in the membrane [4]. Cysteines are conserved in all defensins. The highly conserved Gly (position 12 in Psd1) is present in all plant defensins. Among the residues that compose the interacting Loop1, the Gly12 contributed to the plasticity of the loop and is probably essential for the recognition process. A conserved residue with thermal flexibility may be a key feature maintained by evolution.

The CMH interacting residue Phe (Phe15 in Psd1) is 50% conserved among plant defensins and alternatively is replaced by bulky hydrophobic residues. The second hit is Leu with 18.5%. If we compare the presence of Phe among defensins of Fabaceae family the conservation increases to 74%. The other interacting residue Thr (Thr16 in Psd1) is not so conserved as Phe15 but is maintained in 26% among all plant defensins. Thr16 is 51% conserved among Fabaceae family. Thr is frequently changed by Ser, which appear at a frequency of 38.5% in the same family. In conclusion, the ability to make hydrogen bonds with the glucosyl group is maintained for 69.5% of the Fabaceae defensins. Based on these results the ability to bind CMH should be a conserved feature within Fabaceae defensins.

Defensins in general tends to show low conservation of primary sequence. This is probably due to different mechanisms of interaction with the membrane. The interaction with the membrane may be only the first cellular target. Afterward, they can get internalized and interact with a cytoplasmic target. Therefore, although the similarity between defensin sequences is small this region can reach high scores in the interacting loops if we compare defensins that share the same membrane target. Similarity is higher among defensins from the same family (Fabaceae). We also found high similarity scores among defensins from Poaceae [4].

4.2. Dynamic properties and membrane interaction

Our data pointed out the importance of Loop1 for Psd1 membrane interaction. The mapping was only effective with the use of dynamic properties upon binding. The chemical shift perturbation for such small protein could only partially identify the specific changes that occurred in the binding site. The accommodation in the membrane led to chemical shift changes in different regions of Psd1.

On the other hand the R2/R1 ratio changed in specific regions of the protein due to differences in conformational exchange. The decrease in R2/R1 ratio in Loop1 was indicative of decrease in conformational exchange upon membrane binding, probably because the membrane stabilized a specific conformation. Other residues showed increased conformational exchange. This is also indicative of transient binding and mapped the same Loop1 and Turn3.

We mapped the same regions in the presence of PC:CMH vesicles and DPC micelles. However, no difference was observed in DPC micelles in the presence or absence of CMH. We believe that the higher protein insertion of Psd1 in micelles hampered the observation of small differences in the interaction in PC and PC:CMH. Our data suggests that the phosphatidylcholine head groups are the major attractor of Psd1 through Coulombic attraction. Psd1 search for specific CMH binding in the membrane surface. The recognition of CMH triggers a conformational change that promote protein insertion in the membrane, possibly through a local destabilization of the membrane that ultimately leads to exposure of hydrophobic aliphatic chains. The protein flips toward the membrane surface leading to interaction of Loop1 and Turn3. Since in micelles there are higher hydrophobic exposure the specific effect was not observed.

Several data in the literature suggest the importance of loop regions for interaction [45,46]. The analysis of protein–protein complexes showed that loop regions are preferred contact points and the frequent presence of aromatic amino acids suggest that their side chain are important probably to restrict the loop conformation in the free state [45,47].

4.3. Conformation selection

In the last ten years a new view of binding and allostery is being deduced from the dynamical behavior of protein in their free states. Frequently, regions that participate in recognition show motions in the timescale of milli- to microseconds. In the case of Psd1, Loop1 and Turn3 showed concerted motion in this timescale. In the free state, these recognition regions (frequently loops) are in equilibrium between two or more conformational states. The process of recognition implies in the stabilization of one of these pre-existent conformational states and selection occurs through population shift toward the bound state. These binding mechanisms are being named conformational selection [14–18]. Here, we showed that conformational selection took place in membrane recognition by Psd1. Binding to the membrane led to decrease in conformational exchange for residues Cys14 and Phe15 and His36. We showed that Phe15 interacted directly to CMH. The construction of mutants will validate the important amino acids for interaction.

Acknowledgments

Thanks are due to Dr. Pedro L. Oliveira (UFRJ, Brazil) for the use of their laboratory facilities and for useful discussions. We also thank R. M. Domingues and Fabricio Cruz for technical assistance. This work was supported by grants from Conselho Nacional de Desenvolvimento Cientıfico e Tecnológico (CNPq), ICGEB-Triestes, Fundação de Amparo a Pesquisa do Estado do Rio de Janeiro Carlos Chagas Filho (FAPERJ-Pensa Rio), Coordenação de Aperfeiçoamento de Pessoal de Nível Superior (CAPES) and National Institute of Structural Biology and Bioimaging (INBEB).

Appendix A. Supplementary data

Supplementary data associated with this article can be found, in the online version, at doi:10.1016/j.bbamem.2009.07.013.

References

[1] B.P.H.J. Thomma, B.P.A. Cammue, K. Thevissen, Plant defensins, Planta 216 (2002) 193–202.
[2] J. Sels, J. Mathys, B.M.A. De Coninck, B. Cammue, M.F.C. De Bolle, Plant pathogenesis-related (PR) proteins: a focus on PR peptides, Plant Physiol. and Biochem. 46 (2008) 941–950.
[3] K.A. Silverstein, W.A. Moskal, H.C. Wu, B.A. Underwood, M.A. Graham, C.D. Town, K.A. VandenBosch, Small cysteine-rich peptides resembling antimicrobial peptides have been underpredicted in plants, Plant J. 51 (2007) 262–280.
[4] V.S. De Paula, G. Razzera, L. Medeiros, C.A. Miyamoto, M.S. Almeida, E. Kurtenbach, F.C.L. Almeida, A.P. Valente, Evolutionary relationship between defensins in the Poaceae family strengthened by the characterization of new sugarcane defensins, Plant Mol, Biol. 68 (2008) 321–335.
[5] F.R. Terras, K. Eggermont, V. Kovaleva, N.V. Raikhel, R.W. Osborn, A. Kester, S.B. Rees, S. Torrekens, F. van Leuven, J. Vanderleyden, Small cysteine-rich antifungal proteins from raddish: their role in host defense, Plant cell 7 (1995) 573–588.
[6] A.G. Gao, S.M. Hakimi, C.A. Mittanck, Y. Wu, B.M. Woerner, D.M. Stark, D.M. Shah, J. Liang, C.M. Rommens, Fungal pathogen protection in potato by expression of plant defensin peptide, Nature Biotechnol. 18 (2000) 1307–1310.
[7] J.F. Marcos, A. Muñoz, E. Pérez-Payá, S. Misra, B. López-Garcia, Identification and rational design of novel antimicrobial peptides for plant protection, Ann. Rev. Phytopathol. 46 (2008) 273–301.
[8] W.W.J. Janisiewicz, I.B. Pereira, M.S. Almeida, D.P. Roberts, M. Wisniewski, E. Kurtenbach, Improved biocontrol of fruit decay fungi with *Pichia pastoris* recombinant strains expressing *Ps*d1 antifungal peptide, Post. Biol. Technol. 47 (2008) 218–225.
[9] A.M. Aerts, I.E.J.A. François, B.P.A. Cammue, K. Thevissen, The mode of antifungal action of plant, insect and human defensins, Cell. Mol. Life Sci. 65 (2008) 2069–2079.
[10] R. Jelinek, S. Kolusheva, Membrane interactions of host-defense peptides studied in model systems, Curr. Protein Pept. Sci. 6 (2005) 103–114.
[11] D. Lobo, I.B. Pereira, L. Fragel-Madeira, L.N. Medeiros, L.M. Cabral, J. Faria, R.C. Campos, R. Linden, E. Kurtenbach, Antifungal *Pisum sativum* defensin one interacts with *Neurospora crassa* cyclin F related to cell cycle, Biochemistry 46 (2007) 987–996.
[12] K. Thevissen, B.P. Cammue, K. Lemaire, J. Winderickx, R.C. Dickson, R.L. Lester, K.K. Ferket, F. Van Even, A.H. Parret, W.F. Broekaert, A gene encoding a sphingolipid biosynthesis enzyme determines the sensitivity of *Saccharomyces cerevisiae* to an antifungal plant defensin from dahlia (*Dahlia merckii*), Proc. Natl. Acad. Sci. U. S. A. 97 (2000) 9531–9536.
[13] K. Thevissen, D.C. Warnecke, I.E. Francois, M. Leipelt, E. Heinz, C. Ott, U. Zahringer, B.P. Thomma, K.K. Ferket, B.P. Cammue, Defensins from insects and plants interact with fungal glucosylceramides, J. Biol. Chem. 279 (2004) 3900–3905.
[14] K. Henzel-Wildman, D. Kern, Dynamic personalities of proteins, Nature 450 (2008) 964–972.
[15] B. Volkman, D. Lipson, D.E. Wemmer, D. Kern, Two-state allosteric behavior in a single-domain signaling protein, Science 295 (2002) 2429–2433.
[16] L.C. James, D.S. Tawfik, Conformational diversity and protein evolution — a 60-year-old hypothesis revisited, Trends Biochem Sci. 28 (2003) 361–368.
[17] N. Tokuriki, F. Stricher, L. Serrano, D.S. Tawfik, How protein stability and new functions trade off, PloS Comp. Biol. 4 (2008) e1000002.
[18] A.P. Valente, C.A. Miyamoto, F.C.L. Almeida, Implications of protein conformational diversity for binding and development of new biological active compounds, Curr. Med. Chem. 13 (2006) 3697–3703.
[19] A.G. Palmer, NMR probes of molecular dynamics: overview and comparison with other techniques, Annu. Rev. Biophys. Biomol. Struct. 30 (2001) 129–155.
[20] R. Brüschweiler, New approaches to the dynamic interpretation and prediction of NMR relaxation data from proteins, Curr. Opin. Struct. Biol. 13 (2003) 175–183.
[21] G. Lipari, A. Szabo, Model-free approach to the interpretation of nuclear magnetic resonance relaxation in macromolecules. 1. Theory and range of validity,, J. Am. Chem. Soc. 104 (1982) 4546–4559.
[22] L.W. Tinoco, A. Da Silva Jr., A. Leite, A.P. Valente, F.C.L. Almeida, NMR structure of PW2 bound to SDS micelles. A tryptophan-rich anticoccidial peptide selected from phage display libraries, J. Biol. Chem. 27 (2002) 3651–3656.
[23] L.W. Tinoco, F. Gomes-Neto, A.P. Valente, F.C. Almeida, Effect of micelle interface on the binding of anticoccidial PW2 peptide, J. Biomol. NMR 39 (2007) 315–322.
[24] C. Cruzeiro-Silva, F. Gomes-Neto, L.W. Tinoco, E.M. Cilli, P.V. Barros, P.A. Lapido-Loureiro, P.M. Bisch, F.C. Almeida, A.P. Valente, Structural biology of membrane-acting peptides: conformational plasticity of anticoccidial peptide PW2 probed by solution NMR, Biochim. Biophys. Acta 1768 (2007) 3182–3192.
[25] A. Da Silva Jr, U. Kawazoe, F.F. Freitas, M.S. Gatti, H. Dolder, R.I. Schumacher, M.A. Juliano, M.J. Da Silva MJ, A. Leite, Avian anticoccidial activity of a novel membrane-interactive peptide selected from phage display libraries, Mol. Biochem. Parasitol. 120 (2002) 53–60.
[26] M.S. Almeida, K.M.S. Cabral, R.B. Zingali, E. Kurtenbach, Characterization of two novel defense peptides from pea (*Pisum sativum*) seeds, Arch. Biochem. Biophys. 378 (2000) 278–286.
[27] M.S. Almeida, K.M.S. Cabral, E. Kurtenbach, F.C.L. Almeida, A.P. Valente, Solution structure of *Pisum sativum* defensin 1 by high resolution NMR: plant defensins, identical backbone with different mechanisms of action, J. Mol. Biol. 315 (2002) 749–757.
[28] K.M.S. Cabral, M.S. Almeida, A.P. Valente, F.C.L. Almeida, E. Kurtenbach, Production of the active antifungal *Pisum sativum* defensin 1 (*Ps*d1) in *Pichia pastoris*: overcoming the inefficiency of the STE13 protease, Protein Express. Purif. 31 (2003) 115–122.
[29] M. Vila-Perello, S. Togno, A. Snchez-Vallet, F. Garca-Olmedo, A. Molina, D. Andreu, A minimalist design approach to antimicrobial agents based on a thionin template, J. Med. Chem. 49 (2006) 448–451.
[30] M. Vila-Perello, A. Sanchez-Vallet, F. Garcıa-Olmedo, A. Molina, D. Andreu, Structural dissection of a highly knotted peptide reveals minimal motif with antimicrobial activity, J. Biol. Chem. 280 (2005) 1661–1668.
[31] W.M. Schaaper, G.A. Posthuma, H.H. Plasman, L. Sijtsma, F. Fant, F.A. Borremans, K. Thevissen, W.F. Broekaert, R.H. Meloen, A. van Amerongen, Synthetic peptides derived from the beta2-beta3 loop of *Raphanus sativus* antifungal protein 2 that mimic the active site, J. Pept. Res. 57 (2001) 409–418.
[32] R.S. Duarte, C.R. Polycarpo, R. Wait, R. Hartmann, E. Barreto-Bergter, Structural characterization of neutral glycosphingolipids from *Fusarium* species, Biochim. Biophys. Acta 1390 (1998) 186–196.
[33] M.J. Hope, M.B. Bally, G. Webb, P.R. Cullis, Production of large unilamellar vesicles by a rapid extrusion procedure. Characterization of size distribution, trapped volume and ability to maintain a membrane potential, Biochim. Biophys. Acta 812 (1985) 55–65.
[34] M. Piotto, V. Saudek, V. Sklenar, Gradient-tailored excitation for single-quantum nmr-spectroscopy of aqueous-solutions, J. Biomol. NMR 2 (1992) 661–666.
[35] V. Sklenar, M. Piotto, R. Leppik, V. Saudek, Gradient-tailored water suppression for $^{1}H–^{15}N$ HSQC experiments optimized to retain full sensitivity, J. Magn. Reson. A 102 (1993) 241–245.
[36] N.A. Farrow, R. Muhandiram, A.U. Singer, S.M. Pascal, C.M. Kay, G. Gish, S.E. Shoelson, T. Pawson, J.D. Forman-Kay, L.E. Kay, Backbone dynamics of a free and a phosphopeptidecomplexed Src homology 2 domain studied by ^{15}N NMR relaxation, Biochemistry 33 (1994) 5984–6003.
[37] H.Y. Carr, E.M. Purcell, Effects of diffusion on free precession in nuclear magnetic resonance experiments, Phys. Rev. 94 (1954) 630–638.
[38] S. Meiboom, D. Gill, Modified spin-echo method for measuring nuclear spin relaxation times, Rev. of Sci. Instrum. 29 (1958) 688–691.
[39] A.G. Palmer, J. Willians, A. McDermott, Nuclear Magnetic Resonance studies of biopolymer dynamics, J. Phys. Chem. 100 (1996) 13293–13310.
[40] A.G. Palmer, C.D. Kroenke, J.P. Loria, Nuclear magnetic resonance methods for quantifying microsecond-to-millisecond motions in biological macromolecules, Methods Enzymol. 339 (2001) 204–238.
[41] T.L. Raguse, E.A. Porter, B. Weisblum, S.H. Gellman, Structure–activity studies of 14-helical antimicrobial β-peptides: probing the relationship between conformational stability and antimicrobial potency, J. Am. Chem. Soc. 124 (2002) 12774–12785.
[42] Z. Wu, D.M. Hoover, D. Yang, C. Boulegue, F. Santamaria, J.J Oppenheim, J. Lubkowski, W Lu, Engineering disulfide bridges to dissect antimicrobial and chemotactic activities of human beta-defensin 3, Proc. Natl. Acad. Sci. U. S. A. 100 (2003) 8880–8885.
[43] V. Dhople, A. Krukemeyer, A. Ramamoorthy, The human beta-defensin-3, an antibacterial peptide with multiple biological functions, Biochim Biophys Acta. 1758 (2006) 1499–1512.
[44] J.P. Powers, A. Tan, A. Ramamoorthy, R.E. Hancock, Solution structure and interaction of the antimicrobial polyphemusins with lipid membranes, Biochemistry 44 (2005) 15504–15513.
[45] M. Buyong, T. Elkayam, H. Wolfson, R. Nussinov, Protein–protein interactions: structurally conserved residues distinguish between binding sites and exposed protein surfaces, Proc. Natl. Acad. Sci. U. S. A. 13 (2003) 5772–5777.
[46] A. Shulman-Peleg, M. Shatsky, R. Nussinov, H.J. Wolfson, Spatial chemical conservation of hot spot interactions in protein–protein complexes, BMC Biology 5 (2007) 43–54.
[47] S.A. Dames, R. Aregger, N. Vajpai, P. Bernado, M. Blackledge, S. Grzesiek, Residual dipolar couplings in short peptides reveal systematic conformational preferences of individual amino acids, J. Am. Chem. Soc. 128 (2006) 13508–13514.